

# Distributed Beamforming for Two-Way DF Relay Cognitive Networks Under Primary–Secondary Mutual Interference

Ali Afana, Ali Ghrayeb, Vahid Reza Asghari, and Sofiéne Affes

**Abstract**—In this paper, we consider collaborative beamforming for a cooperative two-way relay spectrum-sharing system where a pair of secondary transceivers communicates via a set of secondary decode-and-forward (DF) relays in the presence of multiple primary transceivers. Among the available relays, only those that receive the signals reliably participate in the cooperative beamforming process and use network coding to simultaneously transmit the weighted signals to the transceivers. Two practical two-way relaying strategies are investigated, namely, DF-XORing and DF-superposition. The former is based on bitwise-level XORing of the detected signals at the relays, whereas the latter is based on symbolwise-level addition at the relays. For each relaying strategy, we derive general optimal beamforming vectors at the relays to keep the interference inflicted on the primary receivers to a predefined threshold. Employing zero-forcing beamforming as a special case, we present an analytical framework of the performance of the secondary system considering the effect of the primary–secondary mutual cochannel interference (CCI). In particular, we derive closed-form expressions for the outage probability, bit error rate (BER), and achievable sum rates over independent and identically distributed Rayleigh fading channels. Numerical results demonstrate the effectiveness of beamforming in compensating for the cognitive system performance loss due to CCI in addition to mitigating the interference to the primary receivers. Simulation results also show that, when the received signals at the relays are equally weighted, DF-XOR always outperforms both DF-superposition and amplify-and-forward (AF) relaying.

**Index Terms**—Cognitive radio (CR), distributed beamforming, performance analysis, spectrum-sharing systems, two-way relaying.

Manuscript received February 6, 2014; revised May 25, 2014, August 1, 2014, and September 20, 2014; accepted September 24, 2014. Date of publication October 13, 2014; date of current version September 15, 2015. This work was supported by the National Priorities Research Program under Grant 09-126-2-054 from the Qatar National Research Fund (a member of Qatar Foundation). The statements made herein are solely the responsibility of the authors. The review of this paper was coordinated by Prof. Y. Zhou.

A. Afana was with Concordia University, Montreal, QC H4B 1R6, Canada. He is currently with the Faculty of Engineering and Science, Memorial University, St. John's, NL A1C 5S7, Canada (e-mail: askafana@mum.ca).

A. Ghrayeb is with the Department of Electrical and Computer Engineering, Texas A&M University, Doha 23874, Qatar, on leave from Concordia University, Montreal, QC H4B 1R6, Canada (e-mail: ali.ghrayeb@qatar.tamu.edu).

V. R. Asghari and S. Affes are with the Institut National de la Recherche Scientifique (INRS), University of Quebec, Montreal, QC G1K 9A9, Canada (e-mail: vahid@emt.inrs.ca; affes@emt.inrs.ca).

Color versions of one or more of the figures in this paper are available online at <http://ieeexplore.ieee.org>.

Digital Object Identifier 10.1109/TVT.2014.2362571

## I. INTRODUCTION

THE RADIO spectrum is a scarce and valuable resource that is strictly managed by spectrum regulation agencies. In addition, recent reports have shown that most of the licensed spectrum is underutilized. Cognitive radio (CR) is proposed as an efficient means to enhance spectrum utilization [1], [2]. The notion of CR is to allow the secondary users (SUs) to access the spectrum of the primary users (PUs) without harming the quality of service of the latter. Recently, cooperative relaying techniques combined with CR have received considerable interest from the research community since it can further improve the reliability and performance of CR systems. An overview of cooperative relaying in CR networks is given in [3] and references therein. It is worth mentioning that most of the work reported in the literature focused on cooperative one-way relaying communications in CR systems [4]–[6].

To further improve bandwidth efficiency, cooperative two-way relaying has emerged as a promising solution where various relaying strategies have been applied at the relay nodes [7], [8]. Typically, for two users to exchange information via a relay node, four time slots are required. However, one may utilize network coding to bring the number of required time slots down to three or two, depending on the way the two received signals are combined at the relay. At the destinations, a self-interference cancellation process is employed at each destination to extract the intended message [9]–[12]. The two received signals at a relay can be combined based on symbolwise-level superposition or bitwise-level XORing. Thus, cooperative two-way relaying can be incorporated in CR networks to further improve spectrum utilization. Recently, in [13], outage probability expressions for both primary and secondary systems were derived in a cooperative two-way decode-and-forward (DF) relaying system where an SU helps two primary transceivers to communicate with each other. Yang *et al.* in [14] extended the work in [13] for two-way amplify-and-forward (AF) relaying for spectrum-sharing systems. In [15], Ubaidulla and Aissa presented an optimal scheme for power allocation and relay selection in a CR network where a pair of SUs communicate with each other through a group of secondary relays in the presence of a PU. All previous works considered power control techniques to manage the interference reflected on the PUs.

Alternatively, collaborative beamforming has emerged as an effective solution to mitigate the interference in cooperative spectrum-sharing systems [16], [17]. While most of the

existing works focused on distributed beamforming in one-way communication [18], little attention has been paid to distributed beamforming in two-way communication CR systems [19]–[22]. Recently, in [19], the problem of sum-rate maximization with interference constraints at the PU for a multi-antenna AF cognitive two-way relay network was investigated where joint beamforming and power allocation was studied. Safavi *et al.* in [20] considered a similar network model as in [19] but with multiple single-antenna AF relays. They obtained the optimal beamforming coefficients using iterative semidefinite programming (SDP) and bisection search methods with the objective of minimizing the interference at a PU with SU signal-to-interference-plus-noise ratio (SINR) constraints. This scheme suffers from high computational complexity and implementation difficulties. A common assumption among all previous works is that they considered only one PU that coexists with the SUs. In [21], we studied a distributed zero-forcing beamforming (ZFB) method for two-way AF relaying in a spectrum-sharing environment where a comparison between two- and three-time-slot (TS) transmission protocols was investigated. In [22], Wang *et al.* proposed a transceiver design for an overlay cognitive two-way relay networks where a secondary multiantenna relay helps two PUs communicate. Optimal precoders were derived using SDP and second-order cone programming methods. AF and DF with XORing and superposition relay strategies were employed at the secondary relay.

We adopt in this paper collaborative distributed beamforming in a two-way DF-selective relay CR network. We consider a three-TS underlay spectrum-sharing two-way relay network comprising two secondary transceivers communicating with each other via a number of secondary DF relays in the presence of a number of PUs.<sup>1</sup> In the first and second TSs, the first and second transceivers broadcast their signals to all available relays, respectively. In the third TS, only the relays that receive the signals (from both transceivers) reliably are used for relaying and beamforming. Specifically, the selected relays combine the two received signals using physical-layer network coding (XORing or superposition) and employ distributed beamforming to keep the reflected interference at the primary receivers (PU-RXs) to a predefined threshold in addition to improving the performance of the secondary system.

In this paper, we aim to address three main issues: 1) which two-way relaying strategy should be chosen to achieve two-way communication between the two transceivers; 2) how to design the optimal beamforming weights at the secondary relays to maximize the received signal-to-noise ratios (SNRs) at the destinations while the interference to the PU-RXs is constrained to a tolerable threshold; and 3) how to allocate the power at the relays in an efficient way. To this end, we consider two-way relaying strategies: DF-XOR and DF-superposition. For each relaying strategy, we adopt the suboptimal ZFB vectors as a special case of optimal beamforming for tractability at the secondary relays. To analyze the system performance and

compare between the relaying strategies, we present an analytical framework for each relaying strategy under the effect of the primary transmitter's (PU-TXs) cochannel interference (CCI). In particular, we derive closed-form expressions for the end-to-end (E2E) outage probability, bit error rate (BER), and achievable sum rates. To get more insight, we derive asymptotic expressions of the outage and BER performance at high SNRs. We also compare the proposed relaying strategies with the three-TS AF relaying strategy reported in [21]. The analytical and simulation results show that DF-XOR outperforms DF-superposition and AF when fixed power allocation is used at the relays. However, when optimal power allocation is used at the relays, DF-superposition performs similar to DF-XOR, whereas the former outperforms AF. This is attributed to the different weighting of the received signals at the relays where the transceiver with higher transmit power is weighted with a higher weight as compared with the transceiver with lower transmit power. The results also demonstrate the efficacy of combining beamforming and cooperative diversity for compensating for the secondary performance loss due to the CCI.

The rest of this paper is organized as follows. Section II describes the system and channel models. ZFB weight design is described in Section III. Section IV introduces the E2E performance analysis. The numerical results are presented in Section V. Section VI concludes this paper.

*Notations:* Throughout this paper, the Frobenius norm of the vectors is denoted by  $\|\cdot\|$ . The transpose and conjugate transpose operations are denoted by  $(\cdot)^T$  and  $(\cdot)^\dagger$ , respectively.  $|x|$  means the magnitude of a complex number  $x$ .  $\mathcal{CN} \sim (0, 1)$  refers to a complex Gaussian normal random variable with zero mean and unit variance.  $\text{Diag}(\mathbf{x})$  and  $\text{Diag}(\mathbf{X})$  denote a diagonal matrix whose diagonal elements are the elements of vector  $\mathbf{x}$  and matrix  $\mathbf{X}$ , respectively.

## II. SYSTEM AND CHANNEL MODELS

### A. System Model

We consider a two-way relaying system that is composed of two secondary transceivers  $S_j$ ,  $j = 1, 2$  and a set of  $L$  DF secondary relays denoted by  $R_i$  for  $i = 1, 2, \dots, L$  coexisting in the same spectrum band with a primary system consisting of a cluster of  $M$  primary transmitter (PU-TX)– $N$  primary receiver (PU-RX) pairs, as shown in Fig. 1. All nodes are equipped with one antenna. The two SUs wish to exchange information through the secondary relays. It is assumed that there is no direct link between the two SUs. The relay nodes operate in the half-duplex mode, and they use the time-division broadcast protocol during three TSs (TS<sub>*i*</sub>),  $i = 1, 2, 3$  [7]. In TS<sub>1</sub>, based on the channel state information (CSI) from  $S_1$  to the  $n$ th PU-RX, which suffers the most interference caused by  $S_1$  (the strongest interference channel),  $S_1$  adjusts its transmit power under a predefined threshold  $Q_1$  and broadcasts its message to all relays.<sup>2</sup> Similarly, in TS<sub>2</sub>, based on the interference CSI from  $S_2$  to the  $\bar{n}$ th PU-RX, which suffers the most interference

<sup>1</sup>We adopt the three-TS protocol instead of the two-TS protocol for the following reasons: 1) to keep the complexity at the relay low (no self-interference) and 2) to allow different weighting of the received signals at different TSs.

<sup>2</sup>It is assumed that  $S_1$  and  $S_2$  have perfect knowledge of their interference channel power gains, which can be acquired through a spectrum-band manager that mediates between the PUs and SUs [5], [14], [18].

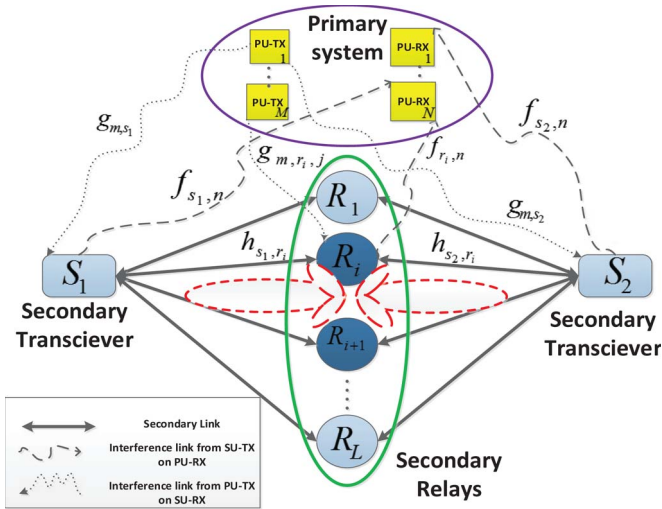


Fig. 1. Spectrum-sharing system with two-way DF relaying.

caused by  $S_2$  (the  $n$ th and  $\bar{n}$ th PU-RXs could be different or the same),  $S_2$  adjusts its transmit power under a predefined threshold  $Q_2$  and broadcasts its message to all relays. In TS<sub>3</sub>, distributed beamforming is applied where ZFB is encompassed as a special case to null the interference from the selected potential relays  $L_s$  (that are eligible to participate) to the  $N$  PU-RXs so that the relays are always able to transmit without interfering with the PU-RXs.

All channel coefficients are assumed to be independent Rayleigh flat fading such that  $|h_{s_j,r_i}|^2$ ,  $|f_{s_j,n}|^2$ ,  $|f_{r_i,n}|^2$ ,  $|g_{m,s_j}|^2$ , and  $|g_{m,r_i,j}|^2$  are exponential distributed random variables with parameters  $\lambda_{s_j,r_i}$ ,  $\lambda_{s_j,n}$ ,  $\lambda_{r_i,n}$ ,  $\lambda_{m,s_j}$ , and  $\lambda_{m,r_i,j}$ , respectively. Let the ZFB vectors  $\mathbf{w}_{\text{zf1}}^T = [w_{11}, w_{12}, \dots, w_{1L_s}]$  be used to direct the signal to  $S_1$  and  $\mathbf{w}_{\text{zf2}}^T = [w_{21}, w_{22}, \dots, w_{2L_s}]$  to direct the signal to  $S_2$ , and  $\mathbf{W}_{\text{zf}}$  is an  $L_s \times L_s$  ZFB processing matrix. Let  $\mathbf{h}_{r_i,s_j}^T = [h_{r_i,s_j,1}, \dots, h_{r_i,s_j,L_s}]$  be the channel vectors between the potential relays and  $S_j$ ,  $j = 1, 2$ . Let  $\mathbf{F}_{\text{rp}}^T = [\mathbf{f}_{\text{r,p1}}, \dots, \mathbf{f}_{\text{r,pN}}]$  be the channel matrix between the relays and all  $N$  PU-RXs, where  $\mathbf{f}_{\text{r,pn}} = [f_{r_1,n}, \dots, f_{r_{L_s},n}]$ .

In the underlying system model, we assume that the transceivers have perfect knowledge of the CSI [7]. In practice, this CSI can be obtained by traditional channel training, estimation, and feedback mechanisms (see, for example, [23] and references therein). Moreover, the transceivers are assumed to have full knowledge of the interference between  $L_s$  relays and PUs, i.e.,  $\mathbf{F}_{\text{rp}}$ . Exploiting the knowledge of the CSI at the transceivers,  $\mathbf{w}_{\text{zf1}}$  and  $\mathbf{w}_{\text{zf2}}$  are designed at  $S_1$  and  $S_2$  and sent back to the relays by only one of the transceivers via low-data-rate feedback links, and that is applicable in slow-fading environments [16], [17]. We acknowledge that obtaining the interference might be a challenging problem in practice.

### B. Transmission Model

As previously mentioned, the communication process occurs over three TSs. In the first time slot, i.e., TS<sub>1</sub>,  $S_1$  transmits, and in the second time slot, i.e., TS<sub>2</sub>,  $S_2$  transmits. As such, when

$S_j$  for  $j = 1, 2$  transmit, the received signal at the  $i$ th relay is given as

$$y_{r_i,j} = \sqrt{P_j} h_{s_j,r_i} x_{s_j} + \sum_{m=1}^M \sqrt{P_{\text{int}}} g_{m,r_i,j} \hat{x}_{im,j} + n_{i,j} \quad (1)$$

where  $P_j$  is the transmit power of  $S_j$ ,  $P_{\text{int}}$  is the interference power inflicted from the PU-TX,  $x_{s_j}$  is the information symbol of  $S_j$ ,  $\hat{x}_{im,j}$  is the  $m$ th PU-TX interfering symbol at the  $i$ th relay, and  $n_{i,j}$  denotes the noise at the  $i$ th relay in the  $j$ th TS. We assume that the transmitted symbols are equiprobable with unit energy. As the secondary relays adopt the DF relaying strategy, they need to decode the signals in TS<sub>1</sub> and TS<sub>2</sub>, respectively. Upon receiving both signals, the set of relays, which can correctly decode both  $x_{s_1}$  and  $x_{s_2}$  by using cyclic redundancy codes, is known as the decoding set  $\mathcal{C}$ . Each relay in the set  $\mathcal{C}$  performs certain processing and then simultaneously forwards the combined signal in the third TS to both transceivers. In the following, we consider the DF-XOR and DF-superposition relaying strategies in our analysis and compare their performances with a performance of three-TS AF relaying in Section V.

1) *XOR Relaying*: In this strategy, each relay combines the received signals from TS<sub>1</sub> and TS<sub>2</sub> by adding the decoded bit sequences exclusively. Let  $\mathbf{b}_{s_j}$  denote the decoded bit sequence from  $x_{s_j}$ , for  $j = 1, 2$ . By applying XOR operation ( $\oplus$ ), the combined bit sequence results in  $\mathbf{b}_{s_{1,2}} = \mathbf{b}_{s_1} \oplus \mathbf{b}_{s_2}$ . Then, the combined bit sequence is encoded, modulated, and weighted as  $L_s \times 1$  signal  $\mathbf{x}_{s_{1,2}} = \mathbf{W}_{\text{zf}} \mathbf{b}_{s_{1,2}}$ . Thus, the received signal at each  $S_j$  is given by

$$y_{s_j,3} = \sqrt{P_r} \mathbf{h}_{r,s_j}^T \mathbf{x}_{s_{1,2}} + \sum_{m=1}^M \sqrt{P_{\text{int}}} g_{m,s_j} \hat{x}_{jm,3} + n_{j,3} \quad (2)$$

where  $P_r$  is the total transmit power at the relays,  $\hat{x}_{jm,3}$  is the  $m$ th PU-TX interfering symbol at  $S_j$ , and  $n_{j,3}$  denotes the noise at each  $S_j$  in TS<sub>3</sub>. Each  $S_j$  can demodulate the received signal and then XOR it with its own transmit bits to obtain the desired data.

Therefore, the corresponding total received SINR at  $S_j$  given  $\mathcal{C}$ , which is denoted as  $\gamma_{s_j|\mathcal{C}}^\oplus$ , is given by

$$\gamma_{s_j|\mathcal{C}}^\oplus = \frac{P_r \left| \mathbf{h}_{r,s_j}^T \mathbf{x}_{s_{1,2}} \right|^2}{\sum_{m=1}^M P_{\text{int}} |g_{m,s_j}|^2 + \sigma^2} \quad (3)$$

where  $\sigma^2$  is the noise variance at  $S_j$ .

2) *Superposition Relaying*: If the secondary relays adopt the superposition relaying strategy, each relay weights the received signals (from both sources) and combines them linearly, i.e.,  $\mathbf{x}_{s_{1,2}} = \sqrt{\alpha_1} \mathbf{w}_{\text{zf1}} x_{s_1} + \sqrt{\alpha_2} \mathbf{w}_{\text{zf2}} x_{s_2}$ . Then, the received signal at each  $S_j$  is given by

$$y_{s_j,3} = \sqrt{P_r} \mathbf{h}_{r,s_j}^T (\sqrt{\alpha_1} \mathbf{w}_{\text{zf1}} x_{s_1} + \sqrt{\alpha_2} \mathbf{w}_{\text{zf2}} x_{s_2}) + \sum_{m=1}^M \sqrt{P_{\text{int}}} g_{m,s_j} \hat{x}_{jm,3} + n_{j,3} \quad (4)$$

where  $\alpha_1$  and  $\alpha_2$  are the power allocation parameters such that  $\alpha_1^2 + \alpha_2^2 = 1$ . As each  $S_j$  has perfect knowledge of  $x_{s_j}$ ,  $\mathbf{w}_{zf_j}$ , and  $\mathbf{h}_{r,s_j}^\dagger$ , it subtracts the self-interference term, and therefore, the resultant total received SINR at  $S_j$  given  $\mathcal{C}$ , which is denoted as  $\gamma_{s_j|\mathcal{C}}^+$ , is given by

$$\gamma_{s_j|\mathcal{C}}^+ = \frac{P_r \alpha_j \left| \mathbf{h}_{r,s_j}^\dagger \mathbf{w}_{zf_j} \right|^2}{\sum_{m=1}^M P_{\text{int}} |g_{m,s_j}|^2 + \sigma^2}. \quad (5)$$

*Remark:* If the relay does not have any knowledge of the channels between itself and the transceivers, it chooses  $\alpha_1 = \alpha_2 = 0.5$ . For the case when the  $i$ th relay has some channel knowledge about  $h_{r_i,s_1}$  and  $h_{r_i,s_2}$  (it may learn it during the previous transmission from the transceivers to the  $i$ th relay in the slow-fading environments),  $\alpha_j$  may be optimized such that the sum rate is maximized.

### C. Mathematical Model and Size of $\mathcal{C}$

In the underlay approach of this model,  $S_j$  can utilize the PU's spectrum as long as the interference it generates from the most affected PU-RX remains below the interference threshold  $Q_j$ . For that reason,  $P_j$  is constrained as  $P_j = \min\{Q_j/(\max_{n=1,\dots,N} |f_{s_j,n}|^2), P_{s_j}\}$ , where  $P_{s_j}$  is the maximum transmission power of  $S_j$ , for  $j = 1, 2$  [24]. Hence, the received SINR at the  $i$ th relay in the  $k$ th TS for  $k = 1, 2$  is given as

$$\gamma_{s_j,r_i,k} = \frac{\min\left\{\frac{Q_j}{\max_{n=1,\dots,N} |f_{s_j,n}|^2}, P_{s_j}\right\} |h_{s_j,r_i}|^2}{\sum_{m=1}^M P_{\text{int}} |g_{m,r_i,k}|^2 + \sigma^2}. \quad (6)$$

*Lemma 1:* The cumulative distribution function (cdf) expression of the received SINR at the  $i$ th secondary relay in the  $k$ th TS is derived as

$$\begin{aligned} & F_{\gamma_{s_j,r_i,k}}(x) \\ &= 1 - e^{-\frac{\lambda_{s_j,r_i} \sigma^2 x}{P_{s_j}}} F_T\left(\frac{Q_j}{P_{s_j}}\right) \left(\frac{\lambda_{s_j,r_i} P_{\text{int}} x}{\lambda_{m,r_i,k} P_{s_j}} + 1\right)^{-M} \\ & \quad - \psi \frac{Q_j N \lambda_{s_j,n}}{\lambda_{s_j,r_i} P_{\text{int}} x} \sum_{n=1}^{N-1} \binom{N-1}{n} (-1)^n x e^{-\frac{Q_j}{P_{s_j}} \lambda_{s_j,n} (n+1)} \\ & \quad \times \left[ (-1)^{\kappa-1} \beta^\kappa e^{\beta \mu} Ei[-\beta \mu] \sum_{a=1}^{\kappa} \Gamma(a) (-\beta)^{\kappa-a} \mu^{-a} \right] \end{aligned} \quad (7)$$

where  $F_T(Q_j/P_{s_j}) = (1 - e^{-(\lambda_{s_j,n} Q_j)/P_{s_j}})^N$ ,  $\psi = e^{-(\lambda_{s_j,r_i} \sigma^2 x)/P_{s_j}}$  ( $\lambda_{m,r_i,k}^M / \Gamma(M)$ ),  $\kappa = M - 1$ ,  $\beta = (\sigma^2 / P_{\text{int}}) + ((n+1) \lambda_{s_j,n} Q_j / \lambda_{s_j,r_i} P_{\text{int}} x)$ ,  $\mu = \lambda_{m,r_i,k} + ((\lambda_{s_j,r_i} P_{\text{int}} x) / P_{s_j})$ , and  $Ei[\cdot]$  is the exponential integral defined in [25, Eq. (8.211)].

*Proof:* See Appendix A.

As previously mentioned, we define  $\mathcal{C}$  to be the set of relays that perfectly decode both signals received in TS<sub>1</sub> and TS<sub>2</sub>, which implies that there is no outage at these relays. This

translates to the fact that the mutual information between each  $S_j$  and each  $i$ th relay is above a specified target value. In this case, the potential  $i$ th relay is only required to meet the decoding constraint given as [26]

$$\Pr[R_i \in \mathcal{C}] = \Pr\left[\frac{1}{3} \log_2(1 + \gamma_{s_j,r_i,k}) \geq \frac{R_{\text{th}}}{2}\right], \quad i = 1, \dots, L \quad (8)$$

where  $(1/3)$  is from the message transmission in three TSs, and  $R_{\text{th}}$  denotes the minimum target rate below which outage occurs. By using the binomial distribution, the probability that the size of  $\mathcal{C}$  is equal to  $L_s$ , which is denoted by  $\Pr[|\mathcal{C}| = L_s]$ , becomes

$$\Pr[|\mathcal{C}| = L_s] = \binom{L}{L_s} P_{\text{off}}^{L-L_s} (1 - P_{\text{off}})^{L_s} \quad (9)$$

where  $P_{\text{off}}$  denotes the probability that the relay fails to decode any one of the signals or both the signals and keeps silent in TS<sub>3</sub>. Let  $P_{o_1}$  and  $P_{o_2}$  be the outage probabilities at any  $i$ th relay for a signal transmitted from  $S_1$  and  $S_2$ , respectively, then  $P_{\text{off}}$  is computed as

$$P_{\text{off}} = 1 - (1 - P_{o_1})(1 - P_{o_2}) \quad (10)$$

where  $P_{o_j}$  for  $j = 1, 2$  can be computed from (7) as

$$P_{o_j} = F_{\gamma_{s_j,r_i,k}}(\gamma_{\text{th}}) \quad (11)$$

where  $\gamma_{\text{th}} = 2^{(3/2)R_{\text{th}}} - 1$  is the SINR threshold at the  $i$ th relay in the  $k$ th TS.

### III. OPTIMAL BEAMFORMING WEIGHTS DESIGN

Our objective here is to maximize the received SNRs at the two transceivers to enhance the performance of the secondary system while limiting the interference to the PU receivers to a tolerable level. Mathematically, the problem formulations for finding the optimal weight vector are described as follows:

$$\begin{aligned} & \max_{\mathbf{v}_{\text{opt}_1}, P_v} P_v \left| \mathbf{h}_{r,s_1}^\dagger \mathbf{v}_{\text{opt}_1} \right|^2 \\ & \text{s.t.} : P_v \left| \mathbf{f}_{r,p_i}^\dagger \mathbf{v}_{\text{opt}_1} \right|^2 \leq Q_i \quad \forall i = 1, \dots, N \\ & \quad \|\mathbf{v}_{\text{opt}_1}\|^2 = 1, \quad P_v \leq P_r \end{aligned} \quad (12)$$

$$\begin{aligned} & \max_{\mathbf{v}_{\text{opt}_2}, P_v} P_v \left| \mathbf{h}_{r,s_2}^\dagger \mathbf{v}_{\text{opt}_2} \right|^2 \\ & \text{s.t.} : P_v \left| \mathbf{f}_{r,p_i}^\dagger \mathbf{v}_{\text{opt}_2} \right|^2 \leq Q_i \quad \forall i = 1, \dots, N \\ & \quad \|\mathbf{v}_{\text{opt}_2}\|^2 = 1, \quad P_v \leq P_r. \end{aligned} \quad (13)$$

To solve the given problems, we first find the optimal beamforming vectors  $\mathbf{v}_{\text{opt}_j}$  for  $j = 1, 2$ , and then, the relay transmit power  $P_v$  is found so that the interference constraint is satisfied. We decompose  $\mathbf{v}_{\text{opt}_j}$  as a linear combination of two orthonormal vectors, namely,  $\mathbf{v}_{\text{opt}_j} = \alpha_{v_j} \mathbf{w}_{zf_j} + \beta_{v_j} \mathbf{w}_{o_j}$ , where  $\alpha_{v_j}$  and  $\beta_{v_j}$  are complex valued weights with  $|\alpha_{v_j}|^2 + |\beta_{v_j}|^2 = 1$  to keep  $\|\mathbf{v}_{\text{opt}_j}\|^2 = 1$ .

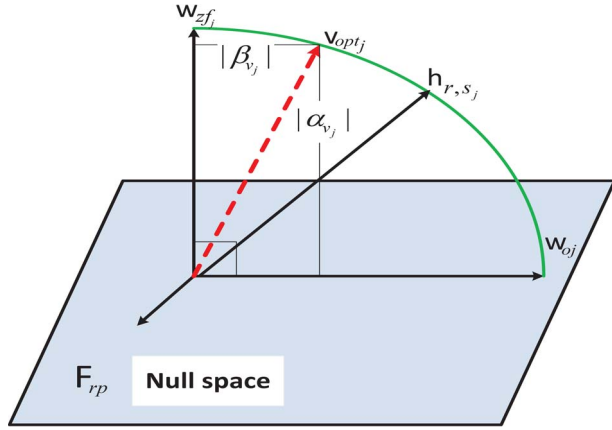


Fig. 2. Geometric explanation of  $\mathbf{v}_{\text{opt}_j}$ .

For the zero-interference constraint case, i.e.,  $Q_i = 0$  for all  $i = 1, \dots, N$ , the optimal beamforming vectors are the ZFB vectors, i.e.,  $\mathbf{v}_{\text{opt}_j} = \mathbf{w}_{\text{zf}_j}$ . According to the ZFB principles,  $\mathbf{w}_{\text{zf}_1}$  and  $\mathbf{w}_{\text{zf}_2}$  are chosen to lie in the orthogonal space of  $\mathbf{F}_{\text{rp}}^\dagger$  such that  $|\mathbf{f}_{\text{r},\text{p}_i}^\dagger \mathbf{w}_{\text{zf}_1}| = 0$  and  $|\mathbf{f}_{\text{r},\text{p}_i}^\dagger \mathbf{w}_{\text{zf}_2}| = 0$ ,  $\forall i = 1, \dots, N$  and  $|\mathbf{h}_{\text{r},\text{s}_1}^\dagger \mathbf{w}_{\text{zf}_1}|$ ,  $|\mathbf{h}_{\text{r},\text{s}_2}^\dagger \mathbf{w}_{\text{zf}_2}|$  are maximized. By applying a standard Lagrangian multiplier method, the weight vectors that satisfy the given optimization methods are given as

$$\mathbf{w}_{\text{zf}_1} = \frac{\mathbf{\Xi}^\perp \mathbf{h}_{\text{r},\text{s}_1}}{\|\mathbf{\Xi}^\perp \mathbf{h}_{\text{r},\text{s}_1}\|}, \quad \mathbf{w}_{\text{zf}_2} = \frac{\mathbf{\Xi}^\perp \mathbf{h}_{\text{r},\text{s}_2}}{\|\mathbf{\Xi}^\perp \mathbf{h}_{\text{r},\text{s}_2}\|} \quad (14)$$

where  $\mathbf{\Xi}^\perp = (\mathbf{I} - \mathbf{F}_{\text{rp}}(\mathbf{F}_{\text{rp}}^\dagger \mathbf{F}_{\text{rp}})^{-1} \mathbf{F}_{\text{rp}}^\dagger)$  is the projection idempotent matrix with rank  $(L_s - N)$  [21]. It can be observed from the rank of the matrix that the cooperative ZBF beamformer becomes effective only when  $L_s > N$ . For the nonzero interference constraint, the secondary relays can increase their transmit power in their own direction, i.e.,  $\mathbf{h}_{\text{r},\text{s}_j}$ . Generally, in this case, the beamforming vector is not in the null space of  $\mathbf{F}_{\text{rp}}$ , and since  $\mathbf{w}_{\text{zf}_j}^\dagger \mathbf{w}_{\text{o}_j} = 0$ , we have

$$\mathbf{w}_{\text{o}_j} = \frac{\mathbf{h}_{\text{r},\text{s}_j} - \mathbf{w}_{\text{zf}_j}^\dagger \mathbf{h}_{\text{r},\text{s}_j} \mathbf{w}_{\text{zf}_j}}{\sqrt{1 - |\mathbf{w}_{\text{zf}_j}^\dagger \mathbf{h}_{\text{r},\text{s}_j}|^2}}. \quad (15)$$

By finding  $\mathbf{w}_{\text{zf}_j}$  and  $\mathbf{w}_{\text{o}_j}$ , the optimal weights are derived as follows.

We have  $P_v |\mathbf{f}_{\text{r},\text{p}_i}^\dagger (\alpha_{v_j} \mathbf{w}_{\text{zf}_j} + \beta_{v_j} \mathbf{w}_{\text{o}_j})|^2 \leq Q_i$ . Since  $\mathbf{f}_{\text{r},\text{p}_i}^\dagger \mathbf{w}_{\text{zf}_j} = 0$ , then  $|\beta_{v_j}| \leq \sqrt{Q_i / (P_v \|\mathbf{f}_{\text{r},\text{p}_i}\|^2 |\mathbf{f}_{\text{r},\text{p}_i}^\dagger \mathbf{w}_{\text{o}_j}|^2)}$  for  $i = 1, \dots, N$ . For a certain value of  $P_v$ ,  $\beta_{v_j}$  is given by  $\beta_{v_j} = \min(\sqrt{Q_i / (\beta_{v_j} \|\mathbf{f}_{\text{r},\text{p}_i}\|^2 |\mathbf{f}_{\text{r},\text{p}_i}^\dagger \mathbf{w}_{\text{o}_j}|^2)})$ ,  $i = 1, 2, \dots, N$  and  $\alpha_{v_j} = (\mathbf{w}_{\text{zf}_j}^\dagger \mathbf{h}_{\text{r},\text{s}_j} / |\mathbf{w}_{\text{zf}_j}^\dagger \mathbf{h}_{\text{r},\text{s}_j}|) \sqrt{1 - \beta_{v_j}^2}$ , and  $P_v \leq P_r$ .

To elaborate, a geometric explanation of  $\mathbf{v}_{\text{opt}_j}$  is given in Fig. 2, where, by rotating  $\mathbf{v}_{\text{opt}_j}$  from the ZFB vector  $\mathbf{w}_{\text{zf}_j}$  toward the maximum ratio transmission (MRT) beamformer  $\mathbf{h}_{\text{r},\text{s}_j} / \|\mathbf{h}_{\text{r},\text{s}_j}\|$ , the secondary relays can maximize the SNR received at the secondary destination at the expense of increasing the interference to the PU while still respecting a predefined

threshold  $Q_i$ . In the case of MRT,  $\mathbf{v}_{\text{opt}_j} = \mathbf{h}_{\text{r},\text{s}_j} / \|\mathbf{h}_{\text{r},\text{s}_j}\|$ , the interference becomes inactive (noncognitive case). Overall, the optimal beamforming vector is given as

$$\mathbf{v}_{\text{opt}_j} = \frac{\mathbf{h}_{\text{r},\text{s}_j} - \mathbf{w}_{\text{zf}_j}^\dagger \mathbf{h}_{\text{r},\text{s}_j} \mathbf{w}_{\text{zf}_j}}{\sqrt{1 - |\mathbf{w}_{\text{zf}_j}^\dagger \mathbf{h}_{\text{r},\text{s}_j}|^2}} + \frac{\mathbf{\Xi}^\perp \mathbf{h}_{\text{r},\text{s}_j}}{\|\mathbf{\Xi}^\perp \mathbf{h}_{\text{r},\text{s}_j}\|}. \quad (16)$$

Although the optimal scheme yields the maximum SNR at the secondary receiver, it is not commonly used due to its intractability, both in terms of design complexity and performance analysis. As an alternative, ZFB may be used for its simplicity and low complexity. For the analysis part, we only consider  $\mathbf{w}_{\text{zf}_j}$  for  $j = 1, 2$  because it enables us to obtain closed-form expressions and get insights on the asymptotic performance of the underlying system.

#### A. XOR Relaying

Since each relay knows its weight coefficients, the ZFB matrix  $\mathbf{W}_{\text{zf}}$  is made up by the diagonal of the product of the two ZFB vectors  $\mathbf{w}_{\text{zf}_1}$  and  $\mathbf{w}_{\text{zf}_2}$ , which is represented as (see [16], [17], and [19] and references therein)

$$\mathbf{W}_{\text{zf}} = \text{Diag}(\mathbf{w}_{\text{zf}_1} \mathbf{w}_{\text{zf}_2}^T). \quad (17)$$

It is worth noting that the weights matrix is diagonal, which guarantees that the relays transmit only their own received signal and that there is no data exchange among the relays. Thus, the algorithm works in a distributed manner.

#### B. Superposition Relaying

The ZFB vectors in superposition relaying are simply chosen to be  $\mathbf{w}_{\text{zf}_1}$  and  $\mathbf{w}_{\text{zf}_2}$ , given by (14) in the first and second TSs, respectively. In the third TS, the weighted received signals are linearly combined with certain power allocation values, as previously described.

### IV. PERFORMANCE ANALYSIS

Here, we examine the performance of the proposed relaying strategies in terms of the outage probability, BER, and achievable sum-rate metrics in the presence of CCIs. As we will see, the derived expressions are cumbersome, and therefore, to get more insights, we derive asymptotic expressions for the outage and BER performance.

#### A. Statistics of the Total Received SINR

Now, after finding  $\mathbf{W}_{\text{zf}}$  in the XOR relaying strategy, we substitute (17) into (3) to get the total received SINR at  $S_j$  given  $\mathcal{C}$ , i.e.,

$$\gamma_{s_j}^\oplus = \frac{P_r \|\mathbf{\Xi}^\perp \mathbf{h}_{\text{r},\text{s}_j}\|^2}{\sum_{m=1}^M P_{\text{int}} |g_{m,s_j}|^2 + \sigma^2}. \quad (18)$$

Similarly, substituting (14) into (5), the total received SINR at  $S_j$  given  $\mathcal{C}$  in the superposition relaying case is given by

$$\gamma_{s_j|c}^+ = \frac{P_r \alpha_j \|\Xi^\perp \mathbf{h}_{r,s_j}\|^2}{\sum_{m=1}^M P_{\text{int}} |g_{m,s_j}|^2 + \sigma^2}. \quad (19)$$

To analyze the system, we first need to obtain the probability density function (pdf) and the cdf of the unconditional total received SINR, i.e.,  $\gamma_{s_j}^*$ , where (\*) refers to (+) or ( $\oplus$ ).

*Lemma 2:* The cdf expression of the total received SINR at  $S_j$  is given by substituting the values of  $\alpha_j = 1$  for the XOR and  $0 < \alpha_j < 1$  for the superposition relaying strategy in the following expression:

$$\begin{aligned} F_{\gamma_{s_j}^*}(x) &= \sum_{L_s=0}^N \binom{L}{L_s} P_{\text{off}}^{L-L_s} (1 - P_{\text{off}})^{L_s} \\ &+ \sum_{L_s=N+1}^L \binom{L}{L_s} P_{\text{off}}^{L-L_s} (1 - P_{\text{off}})^{L_s} \\ &\times \left( 1 - \frac{\lambda_{m,s_j}^M}{\Gamma(M)} \sum_{i=0}^{L_s-N-1} \sum_{k=0}^i \binom{k}{i} P_{\text{int}}^k (\sigma^2)^{i-k} \right. \\ &\left. \times e^{-\frac{\sigma^2 x}{\alpha_j P_r}} \frac{(M-1+k)! x^i}{\left(\lambda_{m,s_j} + \frac{P_{\text{int}} x}{\alpha_j P_r}\right)^{M+k}} \right). \quad (20) \end{aligned}$$

*Proof:* See Appendix B.

The pdf of  $\gamma_{s_j}^*$ , denoted by  $f_{\gamma_{s_j}^*}(\gamma)$ , is simply obtained by differentiating (20). For an interference-limited scenario, i.e.,  $\sigma^2 = 0$ , it is given as

$$\begin{aligned} f_{\gamma_{s_j}^*}(x) &= \sum_{L_s=0}^N \binom{L}{L_s} P_{\text{off}}^{L-L_s} (1 - P_{\text{off}})^{L_s} \delta(x) \\ &+ \sum_{L_s=N+1}^L \binom{L}{L_s} P_{\text{off}}^{L-L_s} (1 - P_{\text{off}})^{L_s} \\ &\times \Gamma[L_s - N + M] \left( \frac{\zeta x^{L_s-N-1}}{\left(\frac{x}{\alpha_j P_r} + \frac{\lambda_{m,s_j}}{P_{\text{int}}}\right)^{L_s-N+M}} \right) \quad (21) \end{aligned}$$

where  $\zeta = (\lambda_{m,s_j})^M / (\Gamma(\varphi) \Gamma(M) P_{\text{int}}^M (\alpha_j P_r)^\varphi)$ , and  $\delta(\cdot)$  is the Dirac function that refers to the received signal-to-interference ratio (SIR) when the relays are inactive. It is plotted in Fig. 3 for various values of  $P_{\text{int}}$ . It clarifies the effect of reducing the interference power from PU-TXs on improving the total received SINR at  $S_j$ . As  $P_{\text{int}}$  decreases, the curve shifts toward the right side, which means that the probability to have a better received SINR for a certain channel condition becomes higher.

In the subsequent sections, we exploit the statistics of the received SINR at both transceivers to investigate the performance of the outage probability, the E2E BER, and the achievable sum-rate metrics.

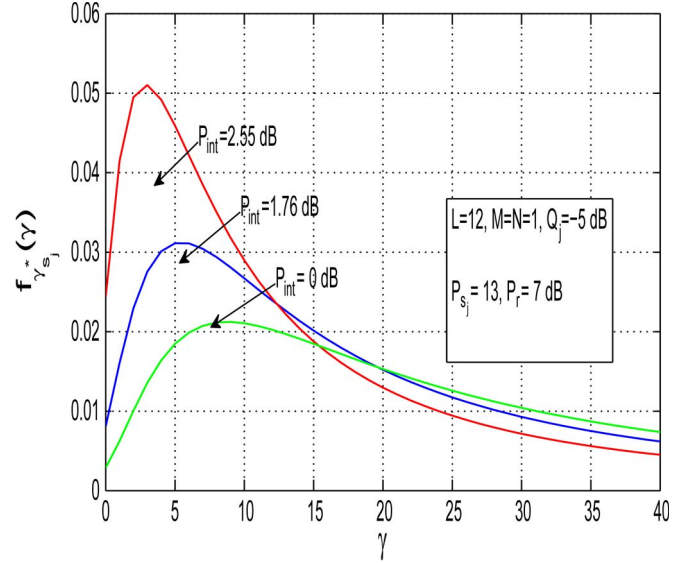


Fig. 3. PDF of the E2E received SIR at  $S_j$ , i.e.,  $f_{\gamma_{s_j}^*}(\gamma)$ .

## B. Outage Probability

An outage event occurs when the total received SINR falls below a certain threshold  $\gamma_{\text{th}}$  and is expressed as  $P_{\text{out}_j^*} = \Pr(\gamma_{s_j}^* < \gamma_{\text{th}})$ . By using (20), the user outage probability of  $S_j$  in a closed form can be written as

$$P_{\text{out}_j^*} = F_{\gamma_{s_j}^*}(\gamma_{\text{th}}). \quad (22)$$

To get more insight on the key parameters, e.g.,  $M$ ,  $N$ ,  $L$ , etc., we derive an approximate expression for the outage probability that shows the behavior of the system at high SINRs.

*Corollary 1:* An asymptotic outage probability expression is given by substituting the values of  $\alpha_j = 1$  for the XOR and  $0 < \alpha_j < 1$  for the superposition relaying strategy in the following expression:

$$\begin{aligned} P_{\text{out}_j^*}^\infty &= \sum_{L_s=0}^N \binom{L}{L_s} \tilde{P}_{\text{off}}^{L-L_s} (1 - \tilde{P}_{\text{off}})^{L_s} \\ &+ \sum_{L_s=N+1}^L \binom{L}{L_s} \tilde{P}_{\text{off}}^{L-L_s} (1 - \tilde{P}_{\text{off}})^{L_s} F_{\gamma_{s_j|c}^*}(\gamma_{\text{th}}) \quad (23) \end{aligned}$$

where  $\tilde{P}_{\text{off}} \approx \sum_{n=0}^{N-1} \binom{N-1}{n} ((-1)^n / (n+1)^2) ((\lambda_{s_j,r_i} M N P_{\text{int}}) / (\lambda_{s_j,p} \lambda_{m,r_i,k} Q_j)) \gamma_{\text{th}} + (1 - e^{-(Q_j / \lambda_{s_j,p} P_{s_j})})^N ((\lambda_{s_j,r_i} M P_{\text{int}}) / (\lambda_{m,r_i,k} P_{s_j})) \gamma_{\text{th}}$ , and  $F_{\gamma_{s_j|c}^*}(\gamma_{\text{th}})$  is given in (36).

*Proof:* See Appendix C.

As can be observed from (23), when the peak interference threshold  $Q_j$  is fixed and the maximum transmit power  $P_{s_j} \rightarrow \infty$ , the outage performance exhibits the error floor at the high SINR. As a conclusion, the diversity order is zero at high SINR, and therefore, the secondary network is more applicable in the low  $P_{s_j}$  values. We also observe from (23) that increasing  $M$  and  $N$  degrades the outage probability. However, increasing  $L$  improves the outage probability.

### C. E2E BER

We analyze the BER performance due to errors occurring at  $S_j$  assuming that all participating relays have accurately decoded and regenerated the message. This probability could be evaluated using the following identity:

$$P_{\text{err}_j^*} = \frac{a\sqrt{b}}{2\sqrt{\pi}} \int_0^{\infty} \frac{e^{-bu}}{\sqrt{u}} F_{\gamma_{s_j}^*}(u) du. \quad (24)$$

Since  $P_{\text{err}_j}$  depends on the modulation scheme, many expressions can be used. For example, binary phase-shift keying (BPSK) is obtained by setting  $(a, b) = (1, 1)$ , whereas quadrature phase-shift keying is attained by setting  $(a, b) = (2, 1/2)$ .

*Theorem 1:* A closed-form expression for a two-way DF relaying strategy with ZFB is given by substituting the values of  $\alpha_j = 1$  and  $0 < \alpha_j < 1$  in the XOR and the superposition relaying strategies, respectively. Thus

$$\begin{aligned} P_{\text{err}_j^*} &= \frac{a}{2} \sum_{L_s=0}^N \binom{L}{L_s} P_{\text{off}}^{L-L_s} (1 - P_{\text{off}})^{L_s} \\ &+ \sum_{L_s=N+1}^L \binom{L}{L_s} P_{\text{off}}^{L-L_s} (1 - P_{\text{off}})^{L_s} \\ &\times \left( \frac{a}{2} - \left( \frac{\sigma^2}{\alpha_j P_r} + b \right)^{-\beta} \left( \frac{P_{\text{int}}}{\alpha_j P_r} \right)^{-(M+k)} \right. \\ &\left. \times \frac{\eta \Phi}{\Gamma(M+k)} G_{2,1}^{1,2} \left( \frac{P_{\text{int}}}{b\alpha_j P_r + \lambda_{m,s_j} \sigma^2} \middle|_{M+k}^{1,1-\beta} \right) \right) \end{aligned} \quad (25)$$

where  $\eta = (P_{\text{int}}/\alpha_j P_r)^{-(M+k)}/\Gamma(M+k)$ ,  $\beta = i - M - k + 0.5$ ,  $\Phi = (a\sqrt{b}/2\sqrt{\pi})(\lambda_{m,s_j}^M/\Gamma(M)) \sum_{i=0}^{L_s-N-1} \sum_{k=0}^i \binom{k}{i} P_{\text{int}}^k (\sigma^2)^{i-k} (M-1+k)!$ , and  $G_{\cdot,\cdot}^{\cdot,\cdot}(\cdot)$  is Meijer's G-function defined in [25, Eq. (9.301)].

*Proof:* See Appendix D.

It is worth noting that Meijer's G-function is implemented in many mathematical softwares such as MATLAB and Mathematica.

Although the expressions in (25) enable numerical evaluation of the exact E2E BER performance, it may not provide useful insights on the effect of key parameters (e.g., the number of secondary relays, the number of PUs, etc.) that influence the system performance. To get more insights, we now introduce an asymptotic BER expression, i.e.,  $P_{s_j} \rightarrow \infty$ , for the DF-XOR and DF-superposition relaying strategies.

*Corollary 2:* An asymptotic BER expression is given by substituting the values of  $\alpha_j = 1$  for the XOR and  $0 < \alpha_j < 1$  for the superposition relaying strategy in the following expression:

$$\begin{aligned} P_{\text{err}_j^*}^{\infty} &= \frac{a}{2} \sum_{L_s=0}^N \binom{L}{L_s} \tilde{P}_{\text{off}}^{L-L_s} (1 - \tilde{P}_{\text{off}})^{L_s} \\ &+ \sum_{L_s=N+1}^L \binom{L}{L_s} \tilde{P}_{\text{off}}^{L-L_s} (1 - \tilde{P}_{\text{off}})^{L_s} I_2 \end{aligned} \quad (26)$$

where  $I_2$  is evaluated in (52).

*Proof:* The proof is similar to the proof of Corollary 1.

Similar to the asymptotic outage probability case, (26) suggests the zero diversity gain with similar conclusions. It is worth noting that the diversity gain of  $(L - N)$  is achieved in the low- $Q_j$  regime. However, if  $P_{s_j}$  is limited, an error floor will occur, and hence, the diversity gain approaches zero at high SINRs. Mathematically, the asymptotic diversity order  $d$  with respect to  $P_{s_j}$  is given by

$$\begin{aligned} d &= \lim_{P_{s_j} \rightarrow \infty} - \frac{\log(P_{\text{err}_j^*}^{\infty})}{\log(P_{s_j})} \\ &= \lim_{P_{s_j} \rightarrow \infty} - \frac{\log(K)}{\log(P_{s_j})} = 0 \end{aligned} \quad (27)$$

where  $K$  is a nonzero constant. Note that  $I_2$  contains Meijer's G-function with  $\lambda_{m,s_j}$ ,  $P_{\text{int}}$ ,  $P_r$ ,  $M$ , and  $\alpha_j$ , which are all constants. Consequently, evaluating  $I_2$  leads to a nonzero constant  $K$ . Hence, the diversity order is zero in the case that  $Q_j$  is fixed, as in (27).

For the second case, that is, for low to medium values of  $P_{s_j}$ , we assume that  $Q_j$  scales with the maximum power level  $P_{s_j}$ , i.e.,  $Q_j = aP_{s_j}$ , which effectively neglects the effect of the interference constraint by allowing for large transmit power. The objective here is to examine the achievable diversity for this range of  $Q_j$ . In this region, we get a diversity gain of the total number of available relays minus the number of primary receivers. This shows that a number of freedom degrees limit the interference inflicted on the  $N$  primary receivers.

### D. Achievable Sum Rate

The achievable sum rate is a substantial performance metric for wireless communications systems because it determines the maximum achievable transmission rate under which the system may adequately function. Specifically, for two-way relaying systems, the achievable sum rate can be expressed as [7], [27], [29]

$$R_{\text{sum}} = \underbrace{\frac{1}{3} \text{E} [\log_2 (1 + \gamma_{s_1}^*)]}_{R_1} + \underbrace{\frac{1}{3} \text{E} [\log_2 (1 + \gamma_{s_2}^*)]}_{R_2}. \quad (28)$$

*Theorem 2:* A closed-form expression for the unconditional achievable rate at  $S_j$  in an interference-limited scenario is given by substituting the values of  $\alpha_j = 1$  and  $0 < \alpha_j < 1$  in the XOR and the superposition relaying strategies, respectively. Thus

$$\begin{aligned} R_j &= \sum_{L_s=N+1}^L \binom{L}{L_s} P_{\text{off}}^{L-L_s} (1 - P_{\text{off}})^{L_s} \bar{\psi} \\ &\times G_{3,3}^{3,2} \left( \frac{P_{\text{int}}}{\lambda_{m,s_j} \alpha_j P_r} \middle|_{L_s-N+M, M, M}^{1, M, 1+M} \right) \end{aligned} \quad (29)$$

where  $\bar{\psi} = (\log_2(e)/3) (((-1)^{-M-1} (\alpha_j P_r)^M) / (\Gamma(\varphi) \Gamma(M) P_{\text{int}}^M))$ . By substituting (29) into (28), we get a closed-form expression of the achievable sum rate of the system.

*Proof:* See Appendix E.

It can be seen from (29) that when the number of the relays is less than the number of primary receivers, i.e.,  $L_s < N$ , the first term of the sum-rate expression disappears because the relays are in inactive mode.

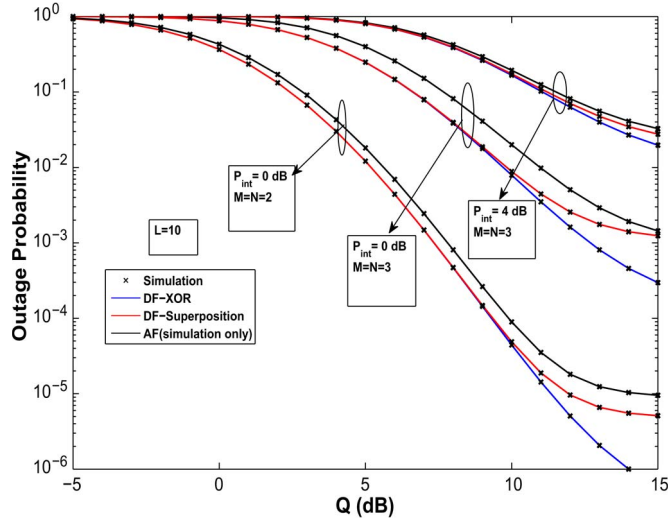


Fig. 4. Outage probability versus  $Q$  (dB) for  $M = N = 2, 3$ ,  $L = 10$ , and different  $P_{\text{int}}$  values.

## V. NUMERICAL RESULTS AND DISCUSSION

Here, we investigate the performance of the derived results through numerical examples and simulations. Unless otherwise stated, let  $d_{S_j, R_i}$  denote the distance from  $S_j$  to the  $i$ th relay, and hence,  $d_{S_1, R_i} = 1 - d_{S_2, R_i}$ . Furthermore, the path-loss exponent is set to 4. We assume that the relays are located on a straight line vertical to the distance between the two sources; however, the results and conclusions of this paper extend to any setting. We further assume that the primary system forms a cluster where PU-TXs are closely located to each other and as all PU-RXs. The distance between the transceivers is equal to one. We also assume that  $\lambda_{s_1, n} = \lambda_{s_2, n} = 1$ ,  $\lambda_{m, s_1} = \lambda_{m, s_2} = 5$ ,  $\lambda_{s_j, r_i} = 1$ , and  $\lambda_{m, r_i, 1} = \lambda_{m, r_i, 2} = 1$ . We also set  $P_r = 5$  dB, the outage threshold as  $\gamma_{\text{th}} = 1$  dB and  $Q_1 = Q_2 = Q$ . We compare the two DF relaying strategies with a three-TS AF relaying strategy proposed in [21]. For a fair comparison, we assume that the total available power at the two transceivers and the relays, i.e.,  $P_{s_j} + P_r \forall j = 1, 2$ , is kept the same for the various relaying strategies. Moreover, we use  $\alpha_1 = \alpha_2 = 0.5$  for a fixed power allocation strategy. We consider a BPSK modulation scheme; however, the derived expressions are general for any higher modulation scheme.

Fig. 4 shows the outage performance of  $S_j$  versus  $Q$  for  $L = 10$ ,  $M = N = 2, 3$  and different values of  $P_{\text{int}} = 0, 4$  dB. As observed from the figure, as the value of  $Q$  increases, the outage performance substantially improves for all curves. Clearly, as the number of existing PU-TX increases from two to three, the outage performance becomes worse as this will increase the sum of the CCI that severely affects the received signals at the transceivers. Furthermore, the figure shows the impact of CCI on the outage performance. As  $P_{\text{int}}$  increases, it degrades the system performance significantly. However, a compensation of this loss in performance is gained by the use of beamforming with cooperative diversity. Comparing between the three strategies, it is seen that the performance of the DF-XOR outperforms the DF-superposition and AF. The reason is that, for the case of the DF-superposition,  $R_i$  transmits  $\mathbf{x}_{s_{1,2}} = \sqrt{\alpha_1} \mathbf{W}_{\text{zf}1} x_{s_1} + \sqrt{\alpha_2} \mathbf{W}_{\text{zf}2} x_{s_2}$ . One of the terms is actually self-

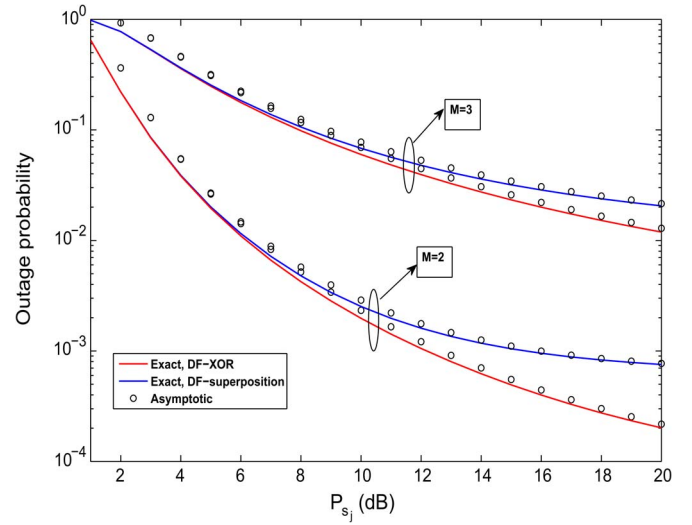


Fig. 5. Asymptotic outage probability versus  $P_{s_j}$  (dB) for  $M = N = 2, 3$ ,  $L = 6$ , fixed  $P_{\text{int}} = 0$  dB, and  $Q_j = -1$  dB.

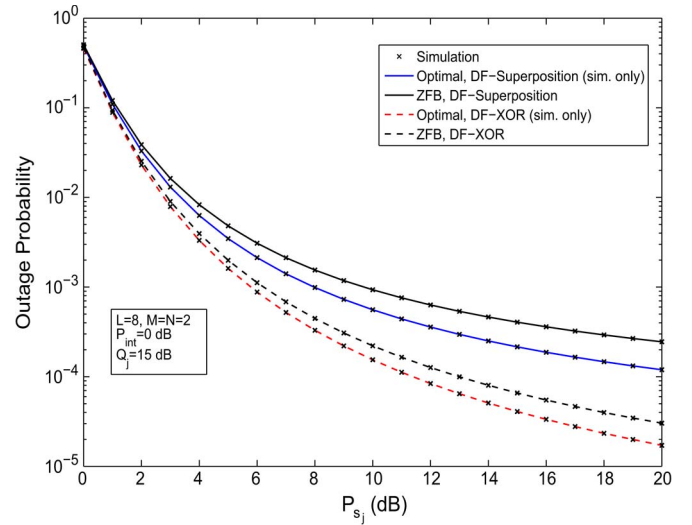


Fig. 6. Outage performance comparison employing ZFB and optimal beamforming vectors for  $M = N = 2$ ,  $L = 8$ , and fixed  $P_{\text{int}} = 0$  dB.

interference to  $S_j$ , and hence, the power used to transmit this term is wasted. However, when DF-XOR is used,  $R_i$  transmits  $\mathbf{x}_{s_{1,2}} = \mathbf{W}_{\text{zf}} \mathbf{b}_{s_{1,2}}$ , and no transmission power is wasted to transmit self-interferences. In the case of AF relaying, the relays do not decode the signals and simply amplify both the signal and the noise, which leads to the worst performance.

In Fig. 5, a plot of the asymptotic outage probability is shown versus  $P_{s_j}$  for both relaying strategies. It shows a good agreement between the exact and asymptotic analytical curves at high SNRs. As predicted by the previous analysis, an error floor occurs at high values of  $P_{s_j}$ , which indicates that the CR networks are only applicable in the low- $P_{s_j}$  region.

In Fig. 6, a comparison between employing the optimal beamforming vector in (16) (simulations only) and ZFB vectors in (14) in terms of outage performance is investigated. For the same transmit power and number of relays and PUs, the results show that there is only a slight difference in the system performance when employing the optimal beamformer versus

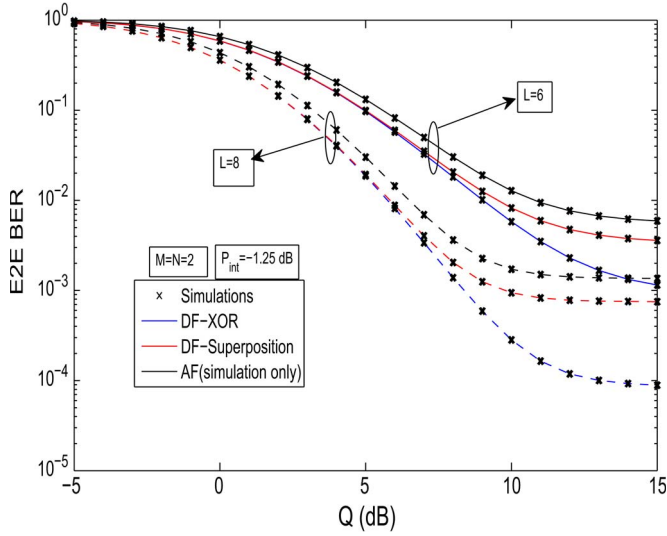


Fig. 7. E2E BER versus  $Q$  (dB) for  $L = 6$ ,  $M = N = 2$ , and different  $P_{int}$  values.

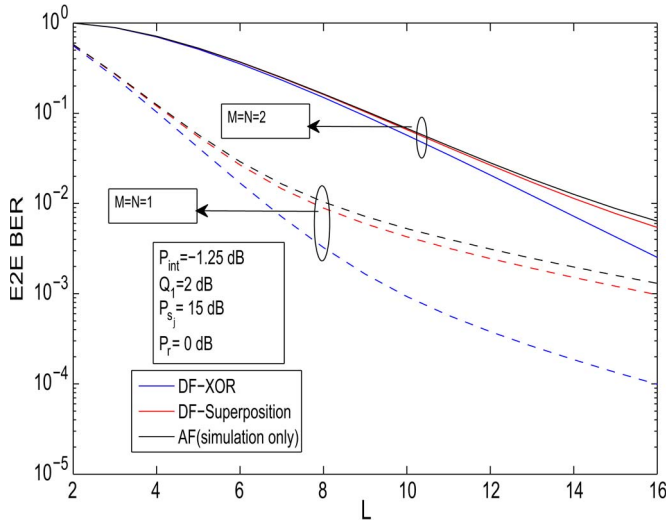


Fig. 8. E2E BER versus  $L$  for  $M = N = 1, 2$  at fixed  $P_{int}$ .

the ZFB as  $Q$  becomes higher. However, the complexity of ZFB is less since it involves only projection to the null space of the interference channel matrix without designing the weight parameters  $\alpha_{v_j}$  and  $\beta_{v_j}$ .

Fig. 7 shows the E2E BER performance versus  $Q$  for  $L = 6, 8$  and  $M = N = 2$ . It is obvious that the BER performance substantially improves as the number of relays increases and  $Q$  becomes looser. This is attributed to the combined cooperative diversity and beamforming, which enhances the total received SNR at the receiver. In addition, it is observed from the BER and outage figures that there is an error floor in the high- $Q$  region, and the curves result in zero diversity. This error flooring is due to the limitations on the secondary transmit power and CCIs. Similar to the outage performance observations, the DF-XOR outperforms both DF-superposition and AF strategies for the aforementioned reasons.

Fig. 8 shows the E2E BER performance versus  $L$  for  $M = N = 1, 2$  at fixed  $P_{int} = -1.25$  dB. As the number of available relays increases, all relaying strategies' performance improves.

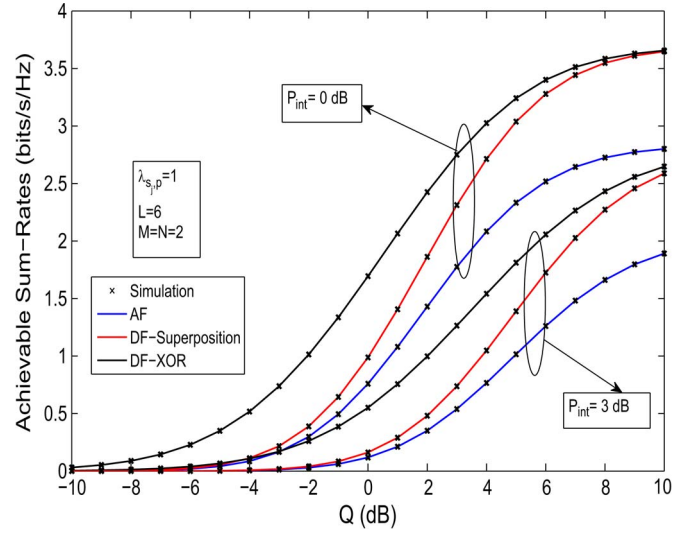


Fig. 9. Achievable sum rates versus  $Q$  (dB) for  $L = 6$ ,  $M = N = 2$ , and different CCI values.

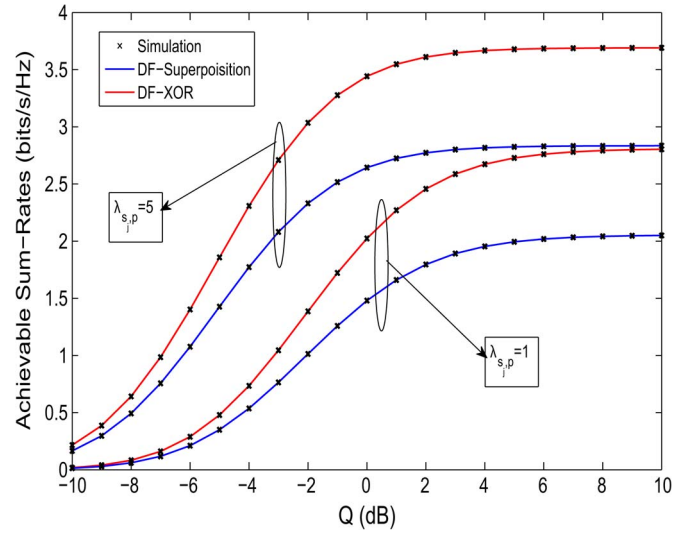


Fig. 10. Achievable sum rates versus  $Q$  (dB) for  $L = 6$ ,  $M = N = 2$  with fixed  $P_{int}$ , and different  $\lambda_{s,p}$  values.

This is due to the reason that the probability of getting more potential relays that succeed in decoding both signals increases, i.e.,  $L_s$  becomes higher, resulting in more participating relays in the beamforming and relaying process. It is also seen that as the number of PU-RXs increases from one to two, the BER performance degrades. Since increasing the number of PU-RXs makes the probability of avoiding the interference on all PU-RXs decrease, which forces the secondary transceivers to transmit with lower power.

In Fig. 9, the achievable sum-rate performance of the secondary system is illustrated for several values of  $P_{int}$  at the same values of  $L = 6$  and  $M = N = 2$ . The CCI effect degrades the performance when it is increased from 0 to 3 dB for all relaying strategies. It can be observed that the DF-XOR sum-rate performance is the best; meanwhile, all of the curves saturate at high values of  $Q_j$  due to the interference constraints.

Fig. 10 shows the achievable sum-rate performance of the secondary system versus  $Q$  for  $L = 6$  and  $M = N = 2$  and

different values of  $P_{\text{int}}$  and fixed  $\lambda_{s_j,p}$ . Again, the same observations as in the previous figures are repeated. Moreover, it is clear that the achievable sum rate increases with  $\lambda_{s_j,p}$  increasing from one to five because as  $\lambda_{s_j,p}$  increases, the quality of the channel between  $S_j$  and PU-RX becomes worse, which reduces the CCI between  $S_j$  and PU-RX. However, when  $\lambda_{s_j,p}$  reaches a certain value, the achievable sum-rate curve saturates due to the constraints on  $P_{s_j}$  and  $Q_j$ .

## VI. CONCLUSION

We have investigated a cooperative two-way DF-selective relaying-based distributed ZFB spectrum-sharing system in the presence of multiple PU-RXs. Two different relaying strategies were considered, and the corresponding optimal weight vectors were designed. The beamforming weights were optimized to maximize the received SNR at both secondary transceivers while the interference inflicted on the PUs is kept to a pre-defined threshold. For each relaying strategy, we analyzed the performance of the secondary system by deriving closed-form expressions for the outage probability, BER, and achievable sum rates. Our numerical results showed that the combination of the distributed ZFB and the cooperative diversity enhances the secondary-link performance by compensating the performance loss due to CCI. Moreover, the results showed that the DF-XOR outperformed DF-superposition and AF relaying strategies when equal power allocation is assumed at the relays while the DF-superposition performance is closer to the DF-XOR when the weighting at the relays is different.

### APPENDIX A PROOF OF LEMMA 1

We derive the cdf of  $\gamma_{s_j,r_i,k} = U/(P_{\text{int}}V + \sigma^2)$ , where  $U = \min\{(Q_j/(\max_{n=1,\dots,N} |f_{s_j,n}|^2)), P_s\} |h_{s_j,r_i}|^2$ , and  $V = \sum_{m=1}^M |g_{m,r_i}|^2$ . By using the definition of cdf of  $\gamma_{s_j,r_i,k}$ , we find

$$F_{\gamma_{s_j,r_i,k}}(x) = \int_0^{\infty} \Pr(U < (P_{\text{int}}y + \sigma^2)x) f_V(y) dy. \quad (30)$$

Since  $V$  is the sum of  $M$  exponential random variables with parameter  $\lambda_{m,r_i}$ , it presents a chi-square random variable with  $2M$  degrees of freedom, and its pdf is given by

$$f_V(y) = \frac{\lambda_{m,r_i}^M y^{M-1} e^{-\lambda_{m,r_i} y}}{\Gamma(M)}. \quad (31)$$

The cdf of  $U$  is given as follows [24]:

$$F_U(x) = 1 - F_T\left(\frac{Q_j}{P_s}\right) - N\lambda_{s_j,n} \sum_{n=1}^{N-1} \binom{N-1}{n} (-1)^n \times \frac{e^{-\frac{Q_j}{P_s}(\lambda_{s_j,n}(n+1) + \frac{\lambda_{s_j,r_i} x}{Q_j})}}{\left(\lambda_{s_j,n}(n+1) + \frac{\lambda_{s_j,r_i} x}{Q_j}\right)} + F_T\left(\frac{Q_j}{P_s}\right) \left(1 - e^{-\frac{\lambda_{s_j,r_i} x}{P_s}}\right) \quad (32)$$

where  $F_T(Q_j/P_s) = F_{\max_{n=1,\dots,N} |f_{s_j,n}|^2}(Q_j/P_s) = (1 - e^{-(\lambda_{s_j,n} Q_j)/P_s})^N$ . Substituting (31) and (32) into (30) and after several algebraic manipulations, (30) is equivalently expressed as

$$F_{\gamma_{s_j,r_i,k}}(x) = 1 - \psi \int_0^{\infty} y^{M-1} e^{-\left(\frac{\lambda_{s_j,r_i} P_{\text{int}} x}{P_s} + \lambda_{m,r_i,k}\right) y} \times \left[ \hat{\psi} \frac{1}{x P_{\text{int}} y + \sigma^2 x + \frac{(n+1)\lambda_{s_j,n} Q_j}{\lambda_{s_j,r_i}}} - F_T\left(\frac{Q_j}{P_s}\right) \right] dy \quad (33)$$

where  $\psi = e^{-(\lambda_{s_j,r_i} \sigma^2 x/P_s)} (\lambda_{m,r_i,k}^M / \Gamma(M))$ , and  $\hat{\psi} = (Q_j/\lambda_{s_j,r_i}) N \lambda_{s_j,n} \sum_{n=1}^{N-1} \binom{N-1}{n} (-1)^n e^{-(Q_j/P_s)\lambda_{s_j,n}(n+1)}$ . After easy simplifications and with the help of [25, Eqs. (3.351.3) and (3.353.5)],  $F_{\gamma_{s_j,r_i,k}}(x)$  is derived as (7), which concludes the proof.

### APPENDIX B PROOF OF LEMMA 2

To analyze the system performance, we first need to obtain the cdf of  $\gamma_{s_j|c}^*$ . Let  $U_1 = P_r \|\Xi^\perp \mathbf{h}_{r,d}\|^2$  and  $V_1 = \sum_{m=1}^M |g_{m,s_j}|^2$  by following the same previous approach, we need the cdf of  $U_1$  and the pdf of  $V_1$ , which can be obtained from [4, Eq. (20)] and (31), respectively. We find the conditional cdf of  $\gamma_{s_j|c}^*$  as

$$F_{\gamma_{s_j|c}^*}(x) = \int_0^{\infty} \frac{\psi_1 \gamma\left(\tau, \frac{(P_{\text{int}} y + \sigma^2)x}{\alpha P_r}\right) y^\kappa e^{-\lambda_{m,s_j} y}}{\Gamma(L_s - N - 1)} dy \quad (34)$$

where  $\psi_1 = \lambda_{m,s_j}^M / \Gamma(M)$ , and  $\tau = L_s - N$ . By representing the incomplete Gamma function into another form utilizing the identities [25, Eqs. (8.352.1) and (1.11)] and after several mathematical manipulations, the integral in (34) is expressed as

$$F_{\gamma_{s_j|c}^*}(x) = 1 - \psi_1 e^{-\frac{\sigma^2 x}{\alpha_j P_r}} \sum_{i=0}^{L_s-N-1} \sum_{k=0}^i \binom{k}{i} P_{\text{int}}^k (\sigma^2)^{i-k} \times x^i \int_0^{\infty} y^{M-1+k} e^{-\left(\lambda_{m,s_j} + \frac{P_{\text{int}} x}{\alpha_j P_r}\right) y} dy. \quad (35)$$

With the help of [25, Eq. (3.3351.3)],  $F_{\gamma_{s_j|c}^*}(x)$  is given as

$$F_{\gamma_{s_j|c}^*}(x) = 1 - \psi_1 \sum_{i=0}^{L_s-N-1} \sum_{k=0}^i \binom{k}{i} P_{\text{int}}^k (\sigma^2)^{i-k} \times e^{-\frac{\sigma^2 x}{\alpha_j P_r}} \frac{(M-1+k)! x^i}{\left(\lambda_{m,s_j} + \frac{P_{\text{int}} x}{\alpha_j P_r}\right)^{M+k}}. \quad (36)$$

To compute the unconditional cdf denoted as  $F_{\gamma_{s_j|c}^*}(x)$ , we use the total probability theorem to get (20), which completes the proof.

APPENDIX C  
PROOF OF COROLLARY 1

From (6), let  $X = |h_{s_j, r_i}|^2$ ,  $Y = \max_{n=1, \dots, N} |f_{s_j, n}|^2$ ,  $Z = \sum_{m=1}^M P_{\text{int}} |g_{m, r_i}|^2$ , and  $\sigma^2 = 0$ , then the cdf of  $\gamma_{s_j, r_i, k}$  conditioned on  $Z$  is given as

$$F_{\gamma_{s_j, r_i, k}|Z}(\gamma) = \underbrace{\Pr\left(\frac{Q_j X}{Y} < Z\gamma, Y \geq \frac{Q_j}{P_{s_j}}\right)}_{I_1(Z)} + \underbrace{\Pr\left(P_{s_j} X < Z\gamma, Y < \frac{Q_j}{P_{s_j}}\right)}_{I_2(Z)}$$

$$I_1(Z) = \int_{\vartheta}^{\infty} f_Y(y) F_X\left(\frac{Z\gamma}{Q_j} y\right) dy \quad (37)$$

where  $\vartheta = Q_j/P_{s_j}$ , and  $f_Y(y) = \lambda_y N \sum_{n=0}^{N-1} \binom{N-1}{n} (-1)^n e^{-(n+1)\lambda_y y}$ .

We approximate the cdf of  $X$  by applying the Taylor series expansion, i.e.,  $F_X(x) = 1 - e^{-(\lambda_x x)}$  is approximated as  $F_X(x) \stackrel{x \rightarrow 0}{\approx} \lambda_x x$ . Using that, we have

$$F_X\left(\frac{Z\gamma}{Q_j} y\right) \stackrel{P_{s_j} \rightarrow \infty}{\approx} \frac{\lambda_x Z\gamma}{Q_j} y. \quad (38)$$

Using the variable change of  $y = ((Q_j/P_{s_j})u)$ , we obtain

$$I_1(Z) \stackrel{P_{s_j} \rightarrow \infty}{\approx} \frac{N\gamma\lambda_x Z}{\lambda_y Q_j} \left( \sum_{n=0}^{N-1} \binom{N-1}{n} \frac{(-1)^n}{(n+1)^2} \right) \times e^{-\frac{\lambda_y(n+1)Q_j}{P_{s_j}}} \left( \frac{\lambda_y(n+1)Q_j}{P_{s_j}} + 1 \right). \quad (39)$$

With further simplification of (39) as  $P_{s_j} \rightarrow \infty$ , it yields

$$I_1(Z) \stackrel{P_{s_j} \rightarrow \infty}{\approx} \frac{\gamma\lambda_x Z}{\lambda_y Q_j} \left( \sum_{n=0}^{N-1} \binom{N-1}{n} \frac{(-1)^n}{(n+1)^2} \right). \quad (40)$$

Next, due to the statistical independence between  $X$  and  $Y$ , the second integral  $I_2(Z)$  is evaluated as

$$I_2(Z) = F_Y(\vartheta) F_X\left(\frac{\gamma}{P_{s_j}} Z\right). \quad (41)$$

Moreover,  $I_2(Z)$  is approximated as

$$I_2(Z) \stackrel{P_{s_j} \rightarrow \infty}{\approx} F_Y(\vartheta) \left(\frac{\gamma}{P_{s_j}} Z\right). \quad (42)$$

The unconditional cdf of  $\gamma_{s_j, r_i, k}$  is derived by averaging  $I_1(Z)$  and  $I_2(Z)$  over the pdf of  $Z$  as follows:

$$F_{\gamma_{s_j, r_i, k}}(\gamma) = \mathbb{E}_Z \left\{ F_{\gamma_{s_j, r_i, k}|Z}(\gamma) \right\} = I_3 + I_4$$

where  $I_3 = \mathbb{E}_Z \{I_1(Z)\}$ , and  $I_4 = \mathbb{E}_Z \{I_2(Z)\}$ . To proceed, we need the pdf of  $Z$ . Because  $Z$  is the sum of  $M$  exponential

random variables with parameter  $P_{\text{int}}$ , it presents a chi-square random variable with pdf given by

$$f_Z(z) = \frac{\lambda_z^M z^{M-1} e^{-\frac{\lambda_z z}{P_{\text{int}}}}}{\Gamma(M) P_{\text{int}}^M}. \quad (43)$$

Next, averaging  $I_1(Z)$  and  $I_2(Z)$  over the pdf of  $Z$ ,  $I_3$ , and  $I_4$  are approximated, respectively, as

$$I_3 \stackrel{P_{s_j} \rightarrow \infty}{\approx} \left( \frac{\lambda_x M N P_{\text{int}}}{\lambda_y \lambda_z Q_j} \right) \left( \sum_{n=0}^{N-1} \binom{N-1}{n} \frac{(-1)^n}{(n+1)^2} \right) \gamma \quad (44)$$

$$I_4 \stackrel{P_{s_j} \rightarrow \infty}{\approx} F_Y(\vartheta) \left( \frac{\lambda_x M P_{\text{int}}}{\lambda_z P_{s_j}} \right) \gamma. \quad (45)$$

Adding (44) and (45) together, we get the asymptotic expression of the cdf of  $\gamma_{s_j, r_i, k}$  as follows:

$$F_{\gamma_{s_j, r_i, k}}(\gamma) \stackrel{P_{s_j} \rightarrow \infty}{\approx} \left( \sum_{n=0}^{N-1} \binom{N-1}{n} \frac{(-1)^n}{(n+1)^2} \right) \times \left( \frac{\lambda_x M N P_{\text{int}}}{\lambda_y \lambda_z Q_j} \right) \gamma + F_Y(\vartheta) \left( \frac{\lambda_x M P_{\text{int}}}{\lambda_z P_{s_j}} \right) \gamma. \quad (46)$$

Computing (46) at  $\gamma = \gamma_{\text{th}}$ , we get

$$\tilde{P}_{\text{off}} \stackrel{P_{s_j} \rightarrow \infty}{\approx} \left( \sum_{n=0}^{N-1} \binom{N-1}{n} \frac{(-1)^n}{(n+1)^2} \right) \frac{\lambda_{s_j, r_i} M N P_{\text{int}}}{\lambda_{s_j, p} \lambda_{m, r_i, k} Q_j} \gamma_{\text{th}} + \left( 1 - e^{-\frac{Q_j}{\lambda_{s_j, p} P_{s_j}}} \right)^N \left( \frac{\lambda_{s_j, r_i} M P_{\text{int}}}{\lambda_{m, r_i, k} P_{s_j}} \right) \gamma_{\text{th}}. \quad (47)$$

By substituting (47) into (22), we get (23). This completes the proof.

APPENDIX D  
PROOF OF THEOREM 1

We divide (24) into two integrals as follows:

$$P_{\text{err}_j}^* = \frac{a\sqrt{b}}{2\sqrt{\pi}} \left( \underbrace{A \int_0^{\infty} \frac{e^{-bx}}{\sqrt{x}} dx}_{I_1} + \underbrace{B \int_0^{\infty} \frac{e^{-bx}}{\sqrt{x}} F_{\gamma_{s_j}^*|c}(x) dx}_{I_2} \right) \quad (48)$$

where  $A = \sum_{L_s=0}^N \binom{L}{L_s} P_{\text{off}}^{L-L_s} (1 - P_{\text{off}})^{L_s}$ , and  $B = \sum_{L_s=N+1}^L \binom{L}{L_s} P_{\text{off}}^{L-L_s} (1 - P_{\text{off}})^{L_s}$ .  $I_1$  is evaluated with the help of [25, Eq. (3.361.2)], which results in  $\sqrt{\pi/b}$ . Next, to compute  $I_2$ , we represent the integrands of  $I_2$  in terms of Meijer's G-functions defined in [25, Eq. (9.301)] using [28, Eqs. (10) and (11)], which are given, respectively, as

$$\left( \lambda_{m, s_j} + \frac{P_{\text{int}} x}{\alpha_j P_r} \right)^{-\nu} = \eta x^{-\nu} G_{1,1}^{1,1} \left( \frac{P_{\text{int}} x}{\lambda_{m d} \alpha_j P_r} \middle| \nu \right) \quad (49)$$

where  $\eta = (P_{\text{int}}/\alpha_j P_r)^{-(M+k)}/\Gamma(M+k)$ , and  $\nu = (M+k)$ . Thus

$$e^{-\left(b + \frac{\sigma^2}{\alpha_j P_r}\right)x} = G_{0,1}^{1,0} \left( \left( b + \frac{\sigma^2}{\alpha_j P_r} \right) x \middle| \nu \right). \quad (50)$$

Thus,  $I_2$  yields

$$I_2 = \frac{a}{2} - \eta \Phi \int_0^\infty x^{-M-k+i-\frac{1}{2}} G_{1,1}^{1,1} \left( \left. \frac{P_{\text{int}} x}{\lambda_{m,s_j} P_r} \right|_{M+k}^1 \right) \times G_{0,1}^{1,0} \left( \left( b + \frac{\sigma^2}{\alpha_j P_r} \right) x \right|_0^- \right) dx \quad (51)$$

where  $\Phi = (a\sqrt{b}/2\sqrt{\pi})(\lambda_{m,s_j}^M/\Gamma(M)) \sum_{i=0}^{L_s-N-1} \sum_{k=0}^i \binom{k}{i} P_{\text{int}}^k (\sigma^2)^{i-k} (M-1+k)!$ . Exploiting the integral of the product of a power term and two Meijer's G-functions [28, Eq. (21)]  $I_2$  results in

$$I_2 = \frac{a}{2} - \frac{\eta \Phi}{\Gamma(M+k)} \left( \frac{P_{\text{int}}}{\alpha_j P_r} \right)^{-(M+k)} \left( \frac{\sigma^2}{\alpha_j P_r} + b \right)^{-\beta} \times G_{2,1}^{1,2} \left( \left. \frac{P_{\text{int}}}{b\alpha_j P_r + \lambda_{m,s_j} \sigma^2} \right|_{M+k}^{1,1-\beta} \right) \quad (52)$$

where  $\beta = i - M - k + 0.5$ . By incorporating the results of  $I_1$  and  $I_2$  into (48), a closed-form expression for the unconditional E2E BER at  $S_j$  is given in (25), which completes the proof.

#### APPENDIX E PROOF OF THEOREM 2

First, we obtain the conditional achievable rate for  $S_j$  by averaging over the conditional pdf in (22), which yields

$$R_{j|c} = \frac{\zeta \Gamma(\varphi + M)}{3} \int_0^\infty \frac{x^{\varphi-1} \log_2(1+x) dx}{\left( \frac{x}{\alpha_j P_r} + \frac{\lambda_{m,s_j}}{P_{\text{int}}} \right)^{\varphi+M}} \quad (53)$$

where  $\varphi = L_s - N$ . Again, expressing the integrand terms in terms of Meijer's G-functions, which are, respectively, given as [28, Eqs. (7), (10), and (11)]

$$\begin{aligned} & \log_2(1+x) \\ &= \log_2(e) G_{2,2}^{1,2} \left( x \right|_{1,0}^{1,1} \right) \\ & x^{\varphi-1} \left( \frac{x}{\alpha_j P_r} + \frac{\lambda_{m,s_j}}{P_{\text{int}}} \right)^{-(\varphi+M)} \\ &= \frac{x^{\varphi-1} \left( \frac{x}{\alpha_j P_r} \right)^{-(\varphi+M)}}{\Gamma(\varphi + M)} G_{1,1}^{1,1} \left( \left. \frac{P_{\text{int}} x}{\lambda_{m,s_j} \alpha_j P_r} \right|_{\varphi+M}^1 \right). \end{aligned} \quad (55)$$

Incorporating (54) and (55) into (53) yields

$$R_{j|c} = \bar{\psi} \int_0^\infty \frac{G_{1,1}^{1,1} \left( \left. \frac{P_{\text{int}} x}{\lambda_{m,s_j} P_r} \right|_{\varphi+M}^1 \right) G_{2,2}^{1,2} \left( x \right|_{1,0}^{1,1} \right)}{x^{M+1}} dx \quad (56)$$

where  $\bar{\psi} = (\log_2(e)/3) (((-1)^{-M-1} (\alpha_j P_r)^M) / (\Gamma(\varphi) \Gamma(M) P_{\text{int}}^M))$ . Again, using [28, Eq. (21)], (56) results in

$$R_{j|c} = \bar{\psi} G_{3,3}^{3,2} \left( \left. \frac{P_{\text{int}}}{\lambda_{m,s_j} \alpha_j P_r} \right|_{L_s, M, M}^{1, M, 1+M} \right). \quad (57)$$

Thus, the unconditional closed-form expression is found as in (29), which completes the proof.

#### REFERENCES

- [1] S. Haykin, "Cognitive radio: Brain-empowered wireless communications," *IEEE J. Sel. Areas Commun.*, vol. 23, no. 9, pp. 201–220, Feb. 2005.
- [2] A. Goldsmith, S. A. Jafar, I. Maric, and S. Srinivasa, "Breaking spectrum gridlock with cognitive radios: An information theoretic perspective," *Proc. IEEE*, vol. 97, no. 5, pp. 894–914, May 2009.
- [3] Q. Zhang, J. Jia, and J. Zhang, "Cooperative relay to improve diversity in cognitive radio networks," *IEEE Commun. Mag.*, vol. 47, no. 2, pp. 111–117, Feb. 2009.
- [4] A. Afana, V. Asghari, A. Ghraryeb, and S. Affes, "Enhancing the performance of spectrum-sharing systems via collaborative distributed beamforming and AF relaying," in *Proc. IEEE GLOBECOM*, Anaheim, CA, USA, Dec. 2012, pp. 1314–1319.
- [5] V. Asghari and S. Aïssa, "Performance of cooperative relaying in spectrum-sharing systems with amplify and forward relaying," *IEEE Trans. Wireless Commun.*, vol. 11, no. 4, pp. 1295–1300, Apr. 2012.
- [6] A. Afana, V. Asghari, A. Ghraryeb, and S. Affes, "On the performance of cooperative relaying spectrum-sharing systems with collaborative distributed beamforming," *IEEE Trans. Commun.*, vol. 62, no. 3, pp. 857–871, Mar. 2014.
- [7] B. Rankov and A. Wittneben, "Spectral efficient protocols for half-duplex fading relay channels," *IEEE J. Sel. Areas Commun.*, vol. 25, no. 2, pp. 379–389, Feb. 2007.
- [8] T. M. Duman and A. Ghraryeb, *Coding for MIMO Communication Systems*. Hoboken, NJ, USA: Wiley, Jan. 2008.
- [9] X. Zeng, A. Ghraryeb, and M. Hasna, "Joint optimal threshold-based relaying and ML detection in network-coded two-way relay," *IEEE Trans. Commun.*, vol. 60, no. 9, pp. 2657–2667, Sep. 2012.
- [10] X. Zhang, M. Hasna, and A. Ghraryeb, "Performance analysis of relay assignment schemes for cooperative networks with multiple source–destination pairs," *IEEE Trans. Wireless Commun.*, vol. 11, no. 1, pp. 166–177, Jan. 2012.
- [11] G. Al-Habian, A. Ghraryeb, M. Hasna, and A. Abu-Dayya, "Threshold-based relaying in coded cooperative networks," *IEEE Trans. Veh. Technol.*, vol. 60, no. 1, pp. 123–135, Jan. 2011.
- [12] S. Nguyen, A. Ghraryeb, G. Al-Habian, and M. Hasna, "Mitigating error propagation in two-way relay channels employing network coding," *IEEE Trans. Wireless Commun.*, vol. 9, no. 11, pp. 3380–3390, Nov. 2010.
- [13] Q. Li, S. H. Ting, A. Pandharipande, and Y. Han, "Cognitive spectrum sharing with two-way relaying systems," *IEEE Trans. Veh. Technol.*, vol. 60, no. 3, pp. 1233–1240, Mar. 2011.
- [14] L. Yang, M. S. Alouini, and K. Qaraqe, "On the performance of spectrum sharing systems with two-way relaying and multiuser diversity," *IEEE Commun. Lett.*, vol. 16, no. 8, pp. 1240–1243, Aug. 2012.
- [15] P. Ubaidulla and S. Aïssa, "Optimal relay selection and power allocation for cognitive two-way relaying networks," *IEEE Wireless Commun. Lett.*, vol. 1, no. 3, pp. 225–228, Jun. 2012.
- [16] V. Havary-Nassab, S. Shahbazpanahi, and A. Grami, "Optimal distributed beamforming for two-way relay networks," *IEEE Trans. Signal Process.*, vol. 58, no. 3, pp. 1238–1250, Mar. 2010.
- [17] M. Zeng, R. Zhang, and S. Cui, "On design of collaborative beamforming for two-way relay networks," *IEEE Trans. Signal Process.*, vol. 59, no. 5, pp. 2284–2295, May 2011.
- [18] R. Manna, R. H. Y. Louie, L. Yonghui, and B. Vucetic, "Cooperative spectrum sharing in cognitive radio networks with multiple antennas," *IEEE Trans. Signal Process.*, vol. 59, no. 11, pp. 5509–5522, Nov. 2011.
- [19] K. Jitvanichphaibool, Y.-C. Liang, and R. Zhang, "Beamforming and power control for multi-antenna cognitive two-way relaying," in *Proc. IEEE WCNC*, 2009, pp. 1–6.
- [20] S. H. Safavi, M. Ardebilipour, and S. Salari, "Relay beamforming in cognitive two-way networks with imperfect channel state information," *IEEE Wireless Commun. Lett.*, vol. 1, no. 4, pp. 344–347, Aug. 2012.
- [21] A. Afana, A. Ghraryeb, V. Asghari, and S. Affes, "Distributed beamforming for spectrum-sharing systems with AF cooperative two-way relaying," *IEEE Trans. Commun.*, vol. 62, no. 9, pp. 3180–3195, Sep. 2014.
- [22] R. Wang, M. Tao, and Y. Liu, "Optimal linear transceiver designs for cognitive two-way relay networks," *IEEE Trans. Signal Process.*, vol. 61, no. 4, pp. 992–1005, Feb. 15, 2013.
- [23] L. Tong, B. M. Sadler, and M. Dong, "Pilot-assisted wireless transmissions: General model, design criteria, signal processing," *IEEE Signal Process. Mag.*, vol. 21, no. 6, pp. 12–25, Nov. 2004.

- [24] Y. Huang, J. Wang, Q. Wu, C. Zhong, and C. Li, "Outage performance of spectrum sharing systems with MRC diversity under multiple primary user's interference," *IEEE Commun. Lett.*, vol. 18, no. 4, pp. 576–579, Feb. 2014.
- [25] I. S. Gradshteyn and I. M. Ryzhik, *Table of integrals series and products*, 7th ed. Amsterdam, The Netherlands: Elsevier, 2007.
- [26] J. Laneman, D. Tse, and G. Wornell, "Cooperative diversity in wireless networks: Efficient protocols and outage behavior," *IEEE Trans. Inf. Theory*, vol. 50, no. 12, pp. 3062–3080, Dec. 2004.
- [27] R. H. Y. Louie, L. Yonghui, and B. Vucetic, "Practical physical layer network coding for two-way relay channels: Performance analysis and comparison," *IEEE Trans. Wireless Commun.*, vol. 9, no. 2, pp. 764–777, Feb. 2010.
- [28] V. Adamchik and O. Marichev, "The algorithm for calculating integrals of hypergeometric type functions and its realization in reduce systems," in *Proc. Int. Conf. Symbolic Algebraic Comput.*, Tokyo, Japan, 1990, pp. 212–224.
- [29] A. Afana, A. Ghraryeb, V. Asghari, and S. Affes, "Collaborative beamforming for spectrum-sharing two-way selective relay networks under co-channel interferences," in *Proc. IEEE PIMRC*, London, U.K., Sep. 2013, pp. 549–553.



**Ali Afana** received the B.Sc. degree in electrical engineering from the Islamic University of Gaza, Gaza, Palestine, in 2006; the M.Sc. degree (with distinction) in communications engineering from Birmingham University, Birmingham, U.K., in 2009; and the Ph.D. degree in electrical engineering from Concordia University, Montréal, QC, Canada, in 2014.

He is currently a Postdoctoral Research Fellow with the Department of Electrical Engineering, Memorial University, St. John's, NL, Canada. His

research interests span different topics in wireless communications, including signal processing for wireless communications, performance analysis of cooperative relaying in cognitive radio networks, and physical-layer security for massive multiple-input–multiple-output systems.



**Ali Ghraryeb** received the Ph.D. degree in electrical engineering from the University of Arizona, Tucson, AZ, USA, in 2000.

He is currently a Professor with the Department of Electrical and Computer Engineering, Texas A&M University, Doha, Qatar (on leave from Concordia University, Montréal, QC, Canada). He is the coauthor of the book *Coding for MIMO Communication Systems* (Wiley, 2008). His research interests include wireless and mobile communications, error-correcting coding, multiple-input–multiple-output systems, wireless cooperative networks, and cognitive radio systems.

Dr. Ghraryeb has instructed/coinstructed technical tutorials at several major IEEE conferences. He served as the Technical Program Committee (TPC) Cochair of the Communications Theory Symposium of the 2011 IEEE Global Communications Conference (Globecom). He is serving as the TPC Cochair of the 2016 IEEE Wireless Communications and Networking Conference. He serves as an Editor for the IEEE TRANSACTIONS ON WIRELESS COMMUNICATIONS and the IEEE TRANSACTIONS ON COMMUNICATIONS. He served as an Associate Editor for the IEEE TRANSACTIONS ON SIGNAL PROCESSING, the IEEE TRANSACTIONS ON VEHICULAR TECHNOLOGY, the Elsevier journal *Physical Communications*, and the Wiley *Wireless Communications and Mobile Computing Journal*. He coreceived the IEEE Globecom Best Paper Award in 2010.



**Vahid Reza Asghari** received the B.Sc. degree in electrical engineering from the Islamic Azad University, Tehran, Iran, in 2002; the M.Sc. degree in telecommunication systems from K.N. Toosi University of Technology, Tehran, in 2005; and the Ph.D. degree in telecommunications from the Energy, Materials and Telecommunications Center of the Institut National de la Recherche Scientifique (INRS-EMT), University of Quebec, Montreal, QC, Canada, in 2012.

From 2005 to 2007, he was a Researcher with the Department of Electrical Engineering, K.N. Toosi University of Technology. From 2011 to 2013, he was a Postdoctoral Research Fellow with the INRS-EMT, where he worked on an admission control algorithm for heterogeneous networks. He is currently a Postdoctoral Research Fellow with the Department of Electrical Engineering, McGill University, Montreal. His research interests include resource scheduling and management and cooperative communications with a focus on heterogeneous systems. He is also interested in behavior modeling, analysis, and management of smart applications using information and communications technology with a focus on cloud computing networks.

Dr. Asghari received the Postdoctoral Research Fellowship Award from the Quebec Government Fonds Qubcois de la Recherche sur la Nature et les Technologies during 2012–2014 and coreceived the Best Paper Award at the IEEE Wireless Communications and Networking Conference in 2010.



**Sofiéne Affes** received the Diplôme d'Ingenieur in telecommunications and the Ph.D. degree (with honors) in signal processing from the École Nationale Supérieure des Télécommunications, Paris, France, in 1992 and 1995, respectively.

He was with the Institut National de la Recherche Scientifique, Montreal, QC, Canada, as a Research Associate until 1997, an Assistant Professor until 2000, and an Associate Professor until 2009. He is currently a Full Professor and the Director of PERWADE: a unique \$4 million research training

program on wireless in Canada involving 27 faculty from eight universities and ten industrial partners.

Dr. Affes received the Discovery Accelerator Supplement Award from the Natural Sciences and Engineering Research Council of Canada from 2008 to 2011 and from 2013 to 2016. From 2003 to 2013, he was the Canada Research Chair in Wireless Communications. In 2006, he served as a General Cochair for the 2006 IEEE Vehicular Technology Conference (VTC)—Fall. In 2008, he received the IEEE VTC Chair Recognition Award from the IEEE Vehicular Technology Society for his exemplary contributions to the success of the IEEE VTC. He also received Best Paper Awards at the 2007 IEEE Global Communications Conference; the 2008 IEEE International Conference on Acoustics, Speech, and Signal Processing; and the 2010 IEEE VTC—Fall. He currently acts as an Associate Editor for the IEEE TRANSACTIONS ON COMMUNICATIONS, the IEEE TRANSACTIONS ON SIGNAL PROCESSING, and the IEEE TRANSACTIONS ON WIRELESS COMMUNICATIONS, as well as for the *Wiley Journal on Wireless Communications and Mobile Computing*.